Nonlinear phonon laser with dissipation-governed levitated optomechanics

Tengfang Kuang
National University of Defense Technology
R. Huang
Hunan Normal University
Wei Xiong
National University of Defense Technology
Yunlan Zuo
Hunan Normal University
Xiang Han
National University of Defense Technology
Franco Nori
RIKEN https://orcid.org/0000-0003-3682-7432
Cheng-Wei Qiu
National University of Singapore https://orcid.org/0000-0002-6605-500X
Hui Luo
National University of Defense Technology
H. Jing
Hunan Normal University
Guangzong Xiao (xiaoguangzong@nudt.edu.cn)
National University of Defense Technology https://orcid.org/0000-0002-6753-9858

Article

Keywords:

Posted Date: January 25th, 2022

DOI: https://doi.org/10.21203/rs.3.rs-1252606/v1

Nonlinear phonon laser with dissipation-governed levitated optomechanics

Tengfang Kuang[1,5], Ran Huang[2,5], Wei Xiong[1], Yunlan Zuo[2], Xiang Han[1], Franco Nori[3], , Chengwei Qiu[4,*], Hui Luo[1,*], Hui Jing[2,*], Guangzong, Xiao[1,*]

[1] College of Advanced Interdisciplinary Studies, NUDT, Changsha Hunan, 410073, China

[2] Department of Physics and Synergetic Innovation Center for Quantum Effects and Applications, Hunan Normal University, Changsha 410081, China

[3] Theoretical Quantum Physics Laboratory, RIKEN Cluster for Pioneering Research, Wako-shi, Saitama 351-0198, Japan

[4] Department of Electrical and Computer Engineering, National University of Singapore, 4 Engineering Drive 3, Singapore, 117576, Singapore

[5] These authors contribute equally to this work

[*]email: chengwei.qiu@nus.edu.sg; luohui.luo@163.com; jinghui73@foxmail.com; xiaoguangzong@nudt.edu.cn.

Phonon lasers, exploiting coherent amplifications of phonons, have been a cornerstone for exploring quantum phononics, imaging nanomaterial structures, and realizing force sensors or phonon frequency combs. Single-mode phonon lasers, governed by dispersive optomechanical coupling, have been recently demonstrated via levitating a nanoparticle using an optical tweezer. Such levitated optomechanical (LOM) devices, with fundamental minimum of noises in high vacuum, can flexibly control large-mass objects with no internal discrete energy levels. However, it is still elusive to realize nonlinear multi-frequency phonon lasing with levitated microscale objects, dominated instead by dissipative LOM coupling due to much stronger optical scattering loss. Here, we report such a nonlinear phonon laser by employing a Yb^{3+}-doped active LOM system. We observe a 3-order of magnitude enhancement for the fundamental-mode phonon lasing, compared with that in its passive counterparts. Above the lasing threshold, higher-order mechanical sidebands emerge spontaneously. Coherent correlations are also identified for the phonon modes. Our gain-assisted dissipative LOM platform no longer relies on any complicated external feedback control.

Our work drives LOM into a new regime where it becomes promising to study mechanical properties or quantum entanglement of typical micro-size objects, such as atmospheric particulates and living cells, and build levitated force sensors with these objects for biomedical or astronomical applications.

Conventional optomechanical systems rely on fixed frames to support mechanical elements, leading to unavoidable energy dissipation and thermal loading at the nanoscale[1]. Levitated optomechanics (LOM), i.e., controlling motions of levitated objects with optical forces[2], have provided unique advantages[3], such as fundamental minimum of damping and noise, the possibility for levitating large and complex objects, as well as high degree of control over both conservative dynamics and coupling to the environment. These advantages are of significance for both fundamental studies of non-equilibrium physics or thermodynamics and applications in metrology[4-11]. In recent years, remarkable achievements have been witnessed in LOM[12-14], such as the realizations of motional ground-state cooling[15,16], room-temperature strong coupling [17], or ultrahigh-precision torque sensing[18], to name only a few. In a very recent work[19], a phonon laser or coherent amplification of phonons, the quanta of vibrations, was demonstrated for a levitated nanosphere, based on dispersive LOM coupling, in which the optical resonance frequency is modulated by mechanical motion. This work offers exciting opportunities of exploring the boundary of classical and quantum worlds with levitated macroscopic objects[16,20,21], as well as making hybrid quantum sensors with levitated spins[22,23]. Nevertheless, sophisticated external feedback controls based on electronic loops[19] are needed to compensate the purely passive optical field, in order to reach the phonon lasing regime. Only single-mode output was observed for phonons above the lasing threshold, without any evidence of nonlinear high-order sidebands.

Except for LOM systems, phonon lasers have also been built by using e.g., semiconductor superlattices[24], nanomagnets[25], single ions[26], and nanomechanical[27] or electromechanical[28] devices. These coherent sound sources, with shorter wavelength of operation than that of a photon laser of the same frequency, are indispensable in steering phonon chips[30], improving the resolution of motional sensors[31], and making nonreciprocal or non-Hermitian devices[32-34]. However, as far as we know, the ability of achieving nonlinear phonon lasers with multiple frequencies, has not been reported. This ability can provide the first step for many important applications such as

mechanical frequency conversion, acoustic frequency combs[35], multi-wave mixing or squeezing of phonons[36-39] and multi-frequency motional sensors.

In this Letter, we develop a strategy to achieve nonlinear phonon lasers for a levitated object at microscales by utilizing an active LOM system. We show that in such a system, dissipative optomechanical coupling[40-43] can be significantly enhanced by introducing an optical gain, thus leading to tunable and efficient multi-frequency phonon lasers. Our system is immune from external feedback control[19] for achieving such phonon lasers, due to the critical role of gain. In fact, for passive systems, only thermal phonons exist for a levitated sphere with the radius $\sim 2\ \mu$m and the mass 1×10^{-4} kg (see Table. 1). To steer this system from a chaotic regime into a phonon lasing regime, we introduce an optical gain to increase the photon lifetime and enhance the photon-phonon coupling, thus achieving *three-order-enhancement* in the power spectrum of the fundamental-mode phonons, with also *30-fold narrowing* in its linewidth. More importantly, above the lasing threshold, we observe higher-order sidebands with double and triple mechanical frequencies, featuring the gain-enhanced nonlinearity in this system.

Table 1| Optomechanical systems for phonon lasing

Features	WGM cavities[33,44]	F-P cavities[37]	Passive LOM[19]	Active LOM
Optical gain	✗	✗	✗	✓
Optomechanical coupling	Dispersive	Dispersive	Dispersive	Dissipative
External feedback	✗	✗	✓	✗
Size of the oscillator	~ 50 μm	~ 1 mm	~ 0.1 μm	~ 2 μm
Mass of the oscillator	~ 10^{-9} kg	~ 10^{-9} kg	~ 10^{-18} kg	~ 10^{-14} kg
Mechanical frequency	10 ~ 100 MHz	~ 100 kHz	~ 100 kHz	~ 10 kHz
Nonlinear sidebands	✗	✗	✗	✓

Notation: WGM, whispering-gallery-mode; F-P, Fabry-Pérot; LOM, Levitated optomechanics; ✓ for Yes; ✗ for No.

New characteristics of our work include the following 3 major points. First, oscillators of the phonon lasers are significantly distinct: the size or the mass of our micro-sphere is 3 or 4 orders larger than the nano-sphere[19], and our LOM systems can thus capture typical micro-size objects and measure their mechanical properties, which is unattainable by nanoscale levitated devices. Second, the physical mechanisms are fundamentally different: our system is governed by the dissipative LOM coupling, due to much stronger optical scattering losses by much larger objects, in contrast to the dispersive LOM coupling in previous works dealing with nanoscale

objects; Third, the nature of phonon lasers are clearly different: we not only demonstrate a fundamental-mode phonon laser, but also observe for the first time coherent higher-order phonon sidebands, including their lasing threshold feature and second-order correlations. In a broader view, our gain-assisted dissipative LOM platform opens the possibility to achieve highly-sensitive LOM control of various micro-size objects, which is of utmost importance for both fundamental studies of macroscopic quantum physics and practical metrology.

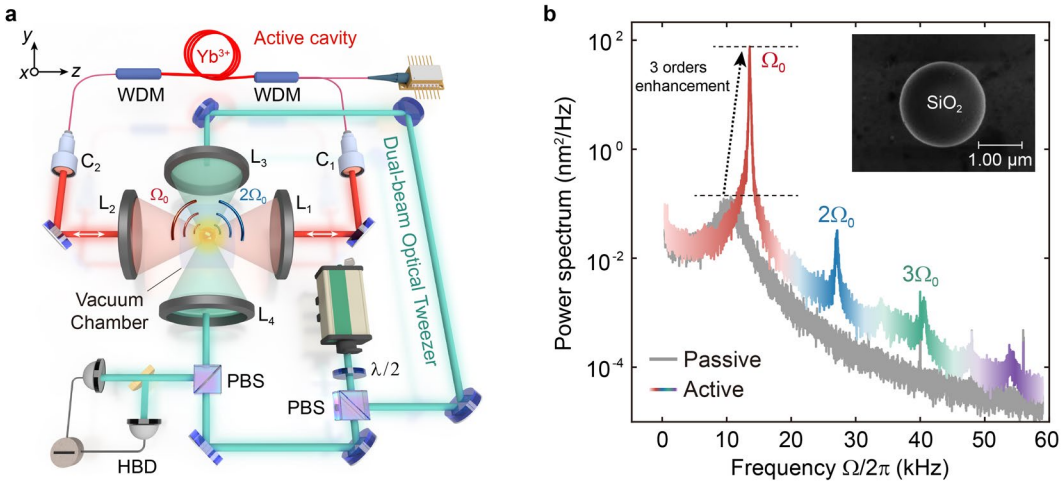

Fig. 1 Experimental overview. a, Schematic diagram of the active levitated optomechanical system, including an active optical cavity (red) and a dual-beam optical tweezer (green). WDM, wavelength division multiplexer; C_1, C_2, collimators; L_1 ~ L_4, lenses; PBS, polarizing beam splitter; HBD, heterodyne balanced detection. **b,** Measured power spectra of phonons in an active cavity (coloured curve) and a passive cavity (grey curve). Inset: Photograph of the levitated microsphere detected with a Scanning Electron Microscope (SEM).

1 μs, which benefits enhanced coherent vibrational amplifications of the sphere. In addition, due to the presence of the optical cavity, our system is free of any need of using complicated feedback control devices[19] (see Supplementary Section 1 for details). As shown in Fig. 1b, essentially different features can be observed in the power spectrums of phonons between our active LOM system and the purely passive system. We see that in the absence of any gain, only thermal phonons can exist; in sharp contrast, three-order-of-magnitude enhancement is achieved in the presence of an

$\Omega_0 = 13.6\,\mathrm{kHz}$.

Moreover, by tuning the pump power, high-order sidebands with mechanical multiple frequencies $2\Omega_0$, $3\Omega_0$, … can also be observed in the spectrum (see also Supplementary Section 1). This enables us to realize a nonlinear multiple-frequency phonon laser in such an active LOM system.

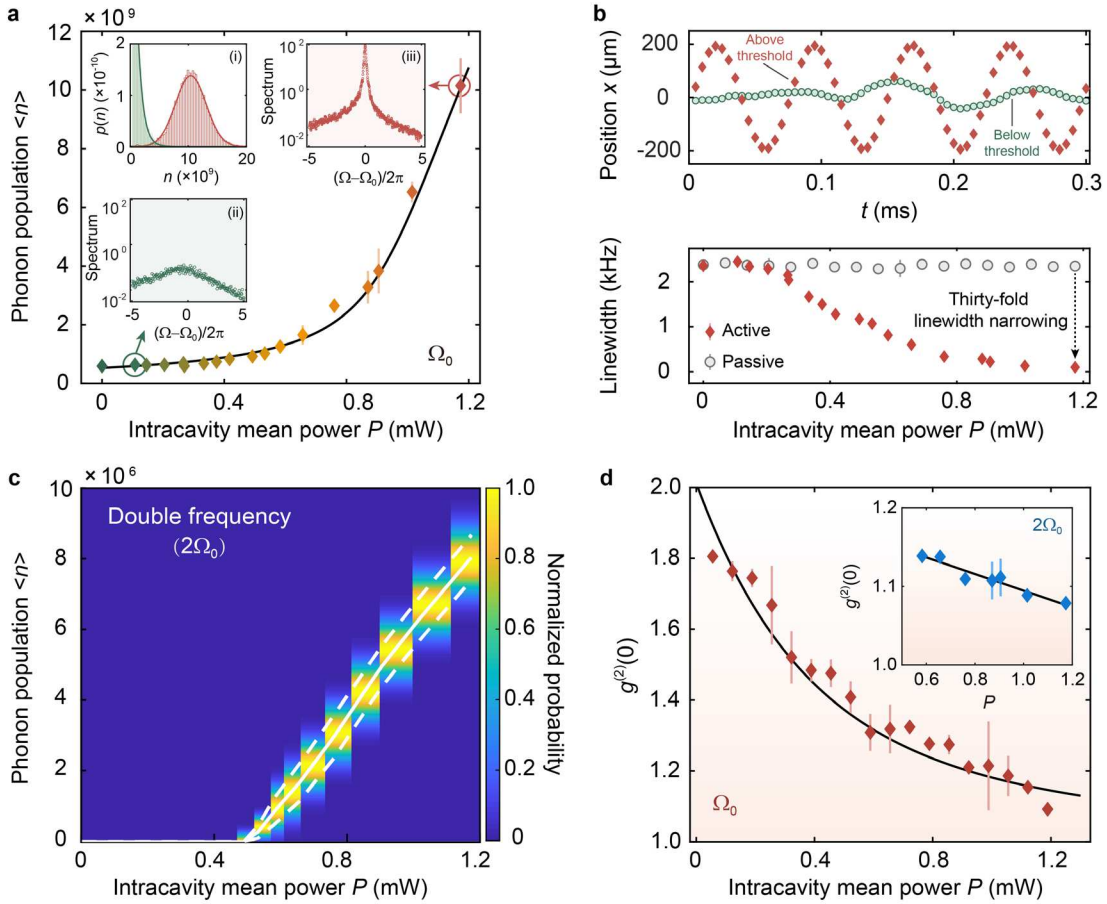

Fig. 2 Experimental results of nonlinear phonon lasers with higher-order sidebands. a, Phonon population with fundamental frequency Ω_0 as a function of intracavity mean power P. The measured threshold power is in good agreement with the theoretical prediction. The insets show (i) the phonon probability distributions, and (ii, iii) the phonon power spectra below and above the oscillation threshold. **b,** Measured oscillation dynamics (upper panel) and linewidths (lower panel) of the fundamental mode by tracing the 2-μm SiO_2 micro-sphere. **c,** Threshold behaviour of the nonlinear phonon laser with double frequency $2\Omega_0$ (white solid curve). The white dashed curves represent ±1 s.d. of each measurement, consisting of 5×10^5 samples. The normalized phonon probability distribution is displayed in colour. **d,** Measured second-order phonon autocorrelation function at zero time delay $g^{(2)}(0)$ versus P for Ω_0. Inset: Measured $g^{(2)}(0)$ with $2\Omega_0$ above the threshold. The solid curves are theoretical results. Error bars represent ±1 s.d. of each measurement, consisting of 5×10^5 samples.

$\langle N\rangle = M\Omega_0\langle x^2\rangle/\hbar$, where M is the mass of the levitated sphere, Ω_0 is the oscillation frequency of the mode, x is the centre of

$\hbar$ is the reduced Planck's constant. Explicit signatures of a lasing threshold can be observed for the fundamental mode with the frequency Ω_0, as shown in Fig. 2a, by increasing the intracavity mean power P. The threshold value is $P_{\mathrm{th}} = 0.37\,\mathrm{mW}$, which agrees well with theoretical calculations (Supplementary Section 2). The insets of Fig. 2a showcase a linewidth narrowing, accompanying the transition from thermal to coherent oscillations. Below the threshold, the oscillator experiences thermal dynamics with mean phonon number 5.89×10^{8}, and the phonon probability distribution is well described by the Boltzmann distribution. By surpassing the lasing threshold, the phonon number is greatly enhanced to 1.02×10^{10} at $P = 1.2\,\mathrm{mW}$, also in conjunction with significant narrowing of linewidth. This is closely related to the fact that the system is switched from spontaneous to stimulated emissions above lasing threshold, resulting in the Gaussian distribution of the generated coherent phonons.

Figure 2b further presents the experimental results of the dynamical behaviours of the sphere. We find that significant vibrational amplifications of the micro-sphere emerge above the lasing threshold. 30-fold improvement in linewidth narrowing is achieved here, compared to purely lossy systems. Clearly, in the passive system, the interaction between the intracavity light and the levitated microsphere is rather weak, due to the large optical loss, that the linewidth remains at about $2.5\,\mathrm{kHz}$. However, when introducing the gain, the linewidth can be significantly modulated by the intracavity power P, and approaches as low as $0.08\,\mathrm{kHz}$ (above the threshold).

Intriguingly, apart from the giant enhancement of fundamental-mode phonon lasing, we also observe spontaneously emerging mechanical higher-order sidebands. Therefore, we reveal the phonon population of the double-frequency mode by filtering out thermal phonons and fundamental-mode phonons. We find similar lasing features for the double-frequency mechanical mode as seen in Fig. 2c, differing from the single-mode phonon laser achieved in the previous works[19,26,28,33,44]. It is also distinguished from the multi-mode phonon laser demonstrated with a flat membrane trapped in a Fabre-Perot cavity[37], in which mode competitions make it only possible to stimulate one single phonon mode into the lasing regime.

$$g^{(2)}(0) = (\langle N^2\rangle - \langle N\rangle)/\langle N\rangle^2$$

, where $\langle N^2\rangle$ is the second moment of this distribution (Fig. 2d). For the lowest-order

Ω_0, we find $g^{(2)}(0)=2$ below the threshold P_{th}, demonstrating the thermal statistics. As P well exceeds P_{th}, $g^{(2)}(0)$ is decreased to 1, which indicates that the phonon dynamics changes from thermal state to coherent state, i.e., the oscillation of the levitated micro-sphere is stimulated into the lasing regime. Moreover, we find $g^{(2)}(0)$ approaches 1 for the nonlinear phonon laser with $2\Omega_0$ when operating in the lasing regime, as shown in the onset of Fig. 2d.

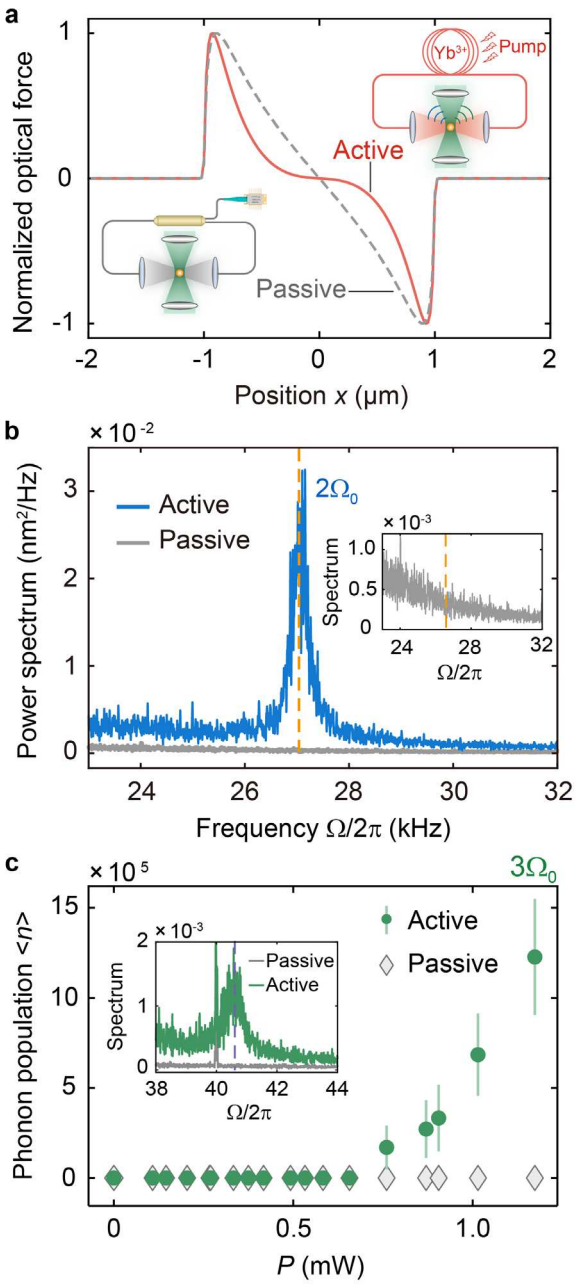

Fig. 3 Optical gain induced nonlinear phonon lasing with double and triple frequencies. a, Normalized optical force distributions for active (red solid curve) and passive (grey dashed curve) setups. The active case shows a strongly nonlinear distribution for the position *x* between -1 μm and 1 μm, while the distribution is linear in the passive case. Insets: Schematic diagrams of the active (upper panel) and passive (lower panel) cases. **b,** Power spectra around $2\Omega_0$ in the active (blue curve) and passive (grey curve) cases. Inset: 30 times magnified spectrum for better view. **c,** Phonon population with the triple frequency $3\Omega_0$ versus the intracavity mean power *P*. Phonon laser with $3\Omega_0$ (green dots) and thermal

phonons (grey curve) are observed in the active and passive cases, respectively. Inset: Power spectra around $3\Omega_0$ in the passive and active cases.

This nonlinear phonon laser results from the anharmonic optical potential produced by the optical-gain-enhanced nonlinearity. Without optical gain, the intracavity light is scattered by the levitated sphere of larger size than that in Ref.[19], leading to a small cavity quality factor and a weak interaction between the cavity field and mechanical oscillator. Therefore, one can find the intracavity optical power P is independent of the x-position of the oscillator (Supplementary Section 3), while the optical force F_{opt}, relying on both of P and x, responds linearly to the position x (Fig. 3a). However, for the active case, the intracavity optical power can be modulated by the mechanical position due to the strong interaction between the light and oscillator. Thus, we can find a strongly nonlinear optical force for the active case, as shown in Fig. 3a. As a result, the double-frequency component emerges in the phonon power spectrum (Fig. 3b). We find a two-order-of-magnitude enhanced amplitude in our active system compared to the conventional passive system with the same intracavity mean power $P = 1.2$ mW. Similar lasing features are also observed for the phonon mode with the triple-frequency $3\Omega_0$ as shown in Fig. 3c, which again cannot be achieved in the absence of optical gain.

In summary, we have experimentally reported nonlinear phonon lasers in active LOM. By introducing optical gain, we have realized a phonon laser on the fundamental mode with three-order-of-magnitude enhancement in the power spectrum, and thirty-fold improvement in linewidth narrowing, without the need of any complicated external feedback control techniques. We also present unequivocal evidence of lasing threshold behaviour, and the phase transition from thermal to coherent phonons by measuring the phonon autocorrelations. More interestingly, for the first time, we observe nonlinear phonon lasers with multiple frequencies, resulting from the optical-gain-enhanced nonlinearity. As far as we know, this is the first observation of such nonlinear mechanical sidebands in LOM systems, which does not rely on the specific material or the shape of the oscillator[45]. We measured also quantum correlations $g^{(2)}(0)$ of sideband phonon lasing for the first time. These results push forward phonon lasers into the nonlinear regime and make many exciting applications more accessible, such as optomechanical combs[35], high-precision metrology, and non-classical state engineering. Our work opens up new perspectives for achieving levitated phonon devices with active LOM, and enables a wide range of applications such as quantum

phononics, multi-frequency mechanical sensors, and high-precision acoustic frequency combs.

Methods

Cavity alignment. We mount the pumping laser to one collimator (Thorlabs, ZC618FC-B), and a power meter to another. The alignment is evaluated by the coupling coefficient from one collimator to another. Through adjusting the lenses and mirrors, the loss of the free-space optical path can be regulated to its lowest value (usually lower than 0.31 dB).

Micro-sphere trapping. The micro-sphere (diameter, 2 μm) was loaded to the trapping region by using an ultrasonic nebulizer, composed of an ultrasonic sheet metal with a great number of 5 μm holes distributed. It was trapped at atmospheric pressure. In most cases, a micro-sphere can be trapped within 30 s. Then, we reduced the pressure to the desired experimental level.

Data availability

The data that support this article are available from the corresponding author upon reasonable request.

References

1. Millen, J., Monteiro, T. S., Pettit, R. & Vamivakas, A. N. Optomechanics with levitated particles. *Rep. Prog. Phys.* **83**, 026401 (2020).
2. Ashkin, A. Acceleration and trapping of particles by radiation pressure. *Phys. Rev. Lett.* **24**, 156-159 (1970).
3. Gonzalez-Ballestero, C., Aspelmeyer, M., Novotny, L., Quidant, R. & Romero-Isart, O. Levitodynamics: Levitation and control of microscopic objects in vacuum. *Science* **374**, eabg3027 (2021).
4. Gieseler, J., Novotny, L., & Quidant, R. Thermal nonlinearities in a nanomechanical oscillator. *Nat. Phys.* **9**, 806-810 (2013).
5. Ranjit, G., Cunningham, M., Casey, K. & Geraci, A. A. Zeptonewton force sensing with nanospheres in an optical lattice. *Phys. Rev. A* **93**, 053801 (2016).
6. Moore, D. C., Rider, A. D. & Gratta, G. Search for millicharged particles using optically levitated microspheres. *Phys. Rev. Lett.* **113**, 251801 (2014).
7. Frimmer, M. et al. Controlling the net charge on a nanoparticle optically levitated in vacuum. *Phys. Rev. A* **95**, 061801 (2017).
8. Jackson Kimball, D. F., Sushkov, A. O. & Budker, D. Precessing ferromagnetic needle magnetometer. *Phys. Rev. Lett.* **116**, 190801 (2016).
9. Monteiro, F. et al. Force and acceleration sensing with optically levitated nanogram masses at microkelvin temperatures. *Phys. Rev. A* **101**, 053835 (2020).
10. Hebestreit, E., Frimmer, M., Reimann, R. & Novotny, L. Sensing static forces with free-falling nanoparticles. *Phys. Rev. Lett.* **121**, 063602 (2018).

11. Rider, A. D. et al. Search for screened interactions associated with dark energy below the 100 μm length scale. *Phys. Rev. Lett.* **117**, 101101 (2016).
12. Chang, D. E. et al. Cavity opto-mechanics using an optically levitated nanosphere. *Proc. Natl. Acad. Sci. U.S.A.* **107**, 1005-1010 (2010).
13. Barker, P. F. & Shneider, M. N. Cavity cooling of an optically trapped nanoparticle. *Phys. Rev. A* **81**, 023826 (2010).
14. Romero-Isart, O., Juan, M. L, Quidant, R. & Cirac, J I. Toward quantum superposition of living organisms. *New J. Phys.* **12**, 033015 (2010).
15. Li, T., Kheifets, S. & Raizen, M. G. Millikelvin cooling of an optically trapped microsphere in vacuum. *Nat. Phys.* **7**, 527-530 (2011).
16. Delić, U. et al. Cooling of a levitated nanoparticle to the motional quantum ground state. *Science* **367**, 892-895 (2020).
17. de los Ríos Sommer, A., Meyer, N. & Quidant, R. Strong optomechanical coupling at room temperature by coherent scattering. *Nat. Commun.* **12**, 276 (2021).
18. Hoang, T. M. et al. Torsional optomechanics of a levitated nonspherical nanoparticle. *Phys. Rev. Lett.* **117**, 123604 (2016).
19. Pettit, R. M. et al. An optical tweezer phonon laser. *Nat. Photon.* **13**, 402-405 (2019).
20. Magrini, L. et al. Real-time optimal quantum control of mechanical motion at room temperature. *Nature* **595**, 373–377 (2021).
21. Tebbenjohanns, F., Mattana, M.L., Rossi, M., Frimmer, M. & Novotny, L. Quantum control of a nanoparticle optically levitated in cryogenic free space. *Nature* **595**, 378–382 (2021).
22. Hoang, T., Ahn, J., Bang, J. & Li, T. Electron spin control of optically levitated nanodiamonds in vacuum. *Nat. Commun.* **7**, 12250 (2016).
23. Gieseler, J. et al. Single-Spin Magnetomechanics with Levitated Micromagnets. *Phys. Rev. Lett.* **124,** 163604 (2020).
24. Trigo, M., Bruchhausen, A., Fainstein, A., Jusserand, B. & Thierry-Mieg, V. Confinement of acoustical vibrations in a semiconductor planar phonon cavity. *Phys. Rev. Lett.* **89**, 227402 (2002).
25. Chudnovsky, E. M. & Garanin, D. A. Phonon superradiance and phonon laser effect in nanomagnets. *Phys. Rev. Lett.* **93**, 257205 (2004).
26. Vahala, K. J. et al. A phonon laser. *Nat. Phys.* **5**, 682-686 (2009).
27. Bargatin, I. & Roukes, M. L. Nanomechanical analog of a laser: amplification of mechanical oscillations by stimulated Zeeman transitions. *Phys. Rev. Lett.* **91**, 138302 (2003).
28. Mahboob, I., Nishiguchi, K., Fujiwara, A. & Yamaguchi, H. Phonon lasing in an electromechanical resonator. *Phys. Rev. Lett.* **110**, 127202 (2013).
29. Li, N. et al. Colloquium: Phononics: Manipulating heat flow with electronic analogs and beyond. *Rev. Mod. Phys.* **84**, 1045-1066 (2012).
30. Hackett, L. et al. Towards single-chip radiofrequency signal processing via acoustoelectric electron–phonon interactions. *Nat. Commun.* **12**, 2769 (2021).
31. Cui, K. et al. Phonon lasing in a hetero optomechanical crystal cavity. *Photonics Res.* **9**, 937-943 (2021).
32. Jing, H. et al. PT-symmetric phonon laser. *Phys. Rev. Lett.* **113**, 053604 (2014).
33. Zhang, J. et al. A phonon laser operating at an exceptional point. *Nat. Photon.* **12**, 479-484 (2018).

34. Jiang, Y., Maayani, S., Carmon, T., Nori, F. & Jing, H. Nonreciprocal phonon laser. *Phys. Rev. Appl.* **10**, 064037 (2018).
35. Ip, M. et al. Phonon lasing from optical frequency comb illumination of trapped ions. *Phys. Rev. Lett.* **121**, 043201 (2018).
36. Mahboob, I., Okamoto, H., Onomitsu, K. & Yamaguchi, H. Two-mode thermal-noise squeezing in an electromechanical resonator. *Phys. Rev. Lett.* **113**, 167203 (2014).
37. Kemiktarak, U., Durand, M., Metcalfe, M. & Lawall, J. Mode competition and anomalous cooling in a multimode phonon laser. *Phys. Rev. Lett.* **113**, 030802 (2014).
38. Fu, W. et al. Phononic integrated circuitry and spin–orbit interaction of phonons. *Nat. Commun.* **10**, 2743 (2019).
39. Benchabane, S. et al. Nonlinear coupling of phononic resonators induced by surface acoustic waves. *Phys. Rev. Appl.* **16**, 054024 (2021).
40. Elste, F., Girvin, S. M. & Clerk, A. A. Quantum noise interference and backaction cooling in cavity nanomechanics. *Phys. Rev. Lett.* **102**, 207209 (2009).
41. Kalantarifard, F. et al. Intracavity optical trapping of microscopic particles in a ring-cavity fiber laser. *Nat. Commun.* **10**, 2683 (2019).
42. Kuang, T. et al. Dual-beam intracavity optical trap with all-optical independent axial and radial self-feedback schemes. *Opt. Express* **29**, 29936 (2021).
43. Leefmans, C. et al. Topological Dissipation in a Time-Multiplexed Photonic Resonator Network. *Nat. Phys.* In press (2022).
44. Grudinin, I. S., Lee, H., Painter, O. & Vahala, K. J. Phonon laser action in a tunable two-level system. *Phys. Rev. Lett.* **104**, 083901 (2010).
45. Asano, M. et al. Observation of optomechanical coupling in a microbottle resonator. *Laser Photonics Rev.* **10**, 603-611 (2016).

Acknowledgements

This work is supported by the National Natural Science Foundation of China (Grants Nos. 61975237, 11904405, 11935006 and 11774086), the Science and Technology Innovation Program of Hunan Province (Grant No. 2020RC4047), Independent Scientific Research Project of National University of Defense Technology (Grant No. ZZKY-YX-07-02), and Scientific Research Project of National University of Defense Technology (Grant No. ZK20-14). F.N. is supported in part by NTT Research, JST [via Q-LEAP, Moonshot R&D, and CREST], JSPS [via KAKENHI], ARO, AOARD, and FQXi. We gratefully acknowledge the valuable assistance from Bin Luo at the BUPT, Yafeng Jiao, Xunwei Xu at HNU, and Zijie Liu, Weiqin Zeng, and Xinlin Chen at NUDT.

Author contributions

G.X. and H.J. conceived the idea. T.K. and G.X. designed the experiments. T.K., W.X. and X.H. performed the experiments and analyzed the experimental data with the help of G.X. R.H. and T.K. performed the theoretical analysis and numerical simulations, guided by H.J. R.H., T.K. and Y.Z. wrote the manuscript with contributions from G.X., H.J., F.N. and C.W.Q. G.X., H.J. and H.L. support the project.

Competing interests

The authors declare no competing interests.

Additional information

Supplementary information is available for this paper at http/

Supplementary Files

This is a list of supplementary files associated with this preprint. Click to download.

- NonlinearphononlaserAppendix.docx
- FigS1.1.png
- FigS1.2.png
- FigS1.3.png
- FigS1.4.png
- FigS3.1.png